CONTROL STRATEGIES FOR A VARIABLE SPEED URBAN WIND TURBINE

A.Naamane, A. Mehdary, M.Trihi*

Laboratoire des Sciences de l'Information et des Systèmes (LSIS)
UMR6168
Avenue escadrille normandie niemen
13397 Marseille cedex 20
*Faculté des sciences aïn chock Casablanca Maroc

Email,: aziz.naamane@lsis.org; adil.mehdary@lsis.org; morad.trihi@fsac.ma

ABSTRACT

Different electric wind power conversion systems structures can be used based on the converters topologies. The main objective in all the structures is always the same: the wind energy at varying wind velocities has to be converted to electric power with the highest performances. In this paper, a double fed induction generator is used with different control strategies: a direct control without taking into account the coupling between the present currents and an indirect control based on state space approach. A comparison in term of robustness and stability between the two methods is presented through simulation results.

Keywords: wind-turbine, double fed induction generator, regulators, Park transform,

1. INTRODUCTION

Today, it is proved that fossil fuels continue to diminish and climate change poses an ever-increasing threat. Among the alternative power sources, wind power "is one of the most promising new energy sources" .Wind is appealing for several reasons. It is abundant, cheap, inexhaustible, widely distributed, clean, and climate-benign, a set of attributes that no other energy source can match. However, there are still many unsolved challenges in expanding wind power. In this paper, two approaches for control of a double fed induction generator (DFIG) are introduced.
Wind turbines use a doubly-fed induction generator (DFIG) consisting of a wound rotor induction generator and an AC/DC/AC IGBT-based PWM converter. The stator winding is connected directly to the 50 Hz grid while the rotor is fed at variable frequency through the AC/DC/AC converter.(Fig.1). The DFIG technology allows extracting maximum energy from the wind for low wind speeds by optimizing the turbine speed, while minimizing mechanical stresses on the turbine during gusts of wind. The optimum turbine speed producing maximum mechanical energy for a given wind speed is proportional to the wind speed. Another advantage of the DFIG technology is the ability for power electronic converters to generate or absorb reactive power, thus eliminating the need for installing capacitor banks as in the case of squirrel-cage induction generator [11].
This paper is organized as follows. Section II presents the modeling of the studied system. In Section III the two control approaches for variable speed wind turbine are presented with the simulation results. Finally, we close the paper by discussing ongoing and future challenges in the last Section.

2. MODELING SYSTEM

2.1. System representation

Figure 1 shows our wind conversion chain, which consists of a turbine, a generator (double fed induction generator) with a rotor winding, converters and PWM (Figure 1).

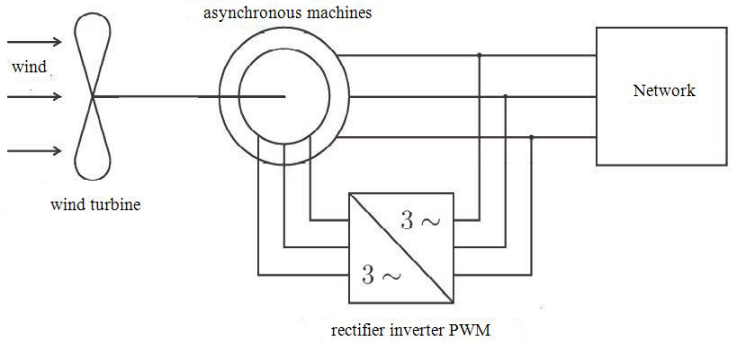

Figure1 : Doubly fed induction generator with converters

2.2. DFIG representation in Park reference

For the different equations used in this paper the following nomenclature will used:
P_m : Mechanical power captured by the wind turbine and transmitted to the rotor
P_s : Stator electrical power output

P_r: Rotor electrical power output
P_{gc}: C grid electrical power output
Q_s : Stator reactive power output
Q_r : Rotor reactive power output
Q_{gc}: C grid reactive power output
T_m: Mechanical torque applied to rotor
T_{em}: Electromagnetic torque applied to the rotor by the generator
ω_r : Rotational speed of rotors
V_s, V_r are Staor and Rotor voltages
V_{qs} , V_{ds} are the three-Phase supply voltages in d-q reference frame, respectively
I_{qs} , I_{ds} are the three-Phase stator currents in d-q reference frame, respectively
V_{qr} , V_{dr} are the three-Phase rotor voltages in d-q reference frame, respectively
I_{qr} , I_{dr} are the three-Phase rotor voltages in d-q reference frame, respectively
R_s, R_r are the stator and rotor resistances of machine per phase, respectively
φ_{qs},φ_{ds} are the three-Phase stator flux linkages in d-q reference frame, respectively
φ_{qr}, φ_{dr} are the three-Phase rotor voltages in d-q reference frame, respectively
L_s , L_r are the leakage inductances of stator and rotor windings, respectively
θ_s, θ_r are the stator and rotor flux angle, respectively

To model the DFIG, we establish the model of a wounded rotor induction machine, which will be obtained in the same manner as the model of squirrel-cage induction generator, except that the rotor voltages are not null.

General equations of synchronous wounded rotor machine are the following [6]:

$$[V_s]_3 = R_s[I_s]_3 + \frac{[d\varphi_s]_3}{dt} \qquad (1)$$
$$[V_r]_3 = R_r[I_r]_3 + \frac{[d\varphi_r]_3}{dt}$$

Using the transformed Park on flux and voltage equations of the DFIG, the model is presented in a two-phase rotating frame, with the following equations: [6] [8].

$$\begin{cases} V_{ds} = R_s I_{ds} + \frac{d\varphi_{ds}}{dt} - \dot{\theta}_s \varphi_{qs} \\ V_{qs} = R_s I_{qs} + \frac{d\varphi_{qs}}{dt} + \dot{\theta}_s \varphi_{ds} \\ V_{dr} = R_r I_{dr} + \frac{d\varphi_{dr}}{dt} - \dot{\theta}_s \varphi_{qr} \\ V_{qr} = R_r I_{qr} + \frac{d\varphi_{qr}}{dt} + \dot{\theta}_r \varphi_{dr} \end{cases} \qquad (2)$$

$$\begin{cases} \varphi_{ds} = L_s I_{ds} + M I_{dr} \\ \varphi_{qs} = L_s I_{qs} + M I_{qr} \\ \varphi_{dr} = L_r I_{dr} + M I_{ds} \\ \varphi_{qr} = L_r I_{qr} + M I_{qs} \end{cases} \qquad (3)$$

The electromagnetic torque is expressed by:

$$\Gamma_{em} = \frac{M}{L_s}(I_{qr}\varphi_{ds} - I_{dr}\varphi_{qs}) \qquad (4)$$

p is the number of pole of the DFIG.

By orienting the reference (d, q) so that the axis is aligned with the stator flux [8] [9], we obtain:

$$\varphi_{ds} = \varphi_s \quad \text{and} \quad \varphi_{qs} = 0 \qquad (5)$$

and the electromagnetic torque expression is:

$$\Gamma_{em} = \frac{M}{L_s} I_{qr} \varphi_s \qquad (6)$$

And the flux equation is:

$$\varphi_s = L_s I_{ds} + M I_{dr} \qquad (7)$$

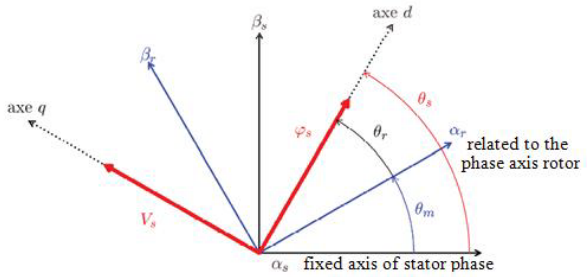

Figure 2: Orientation of the axis of the stator flux

Assuming that the grid voltage remains stable, with the value V_s, and as the flux is considered constant, the electromagnetic torque is proportional to the rotor current I_{qr} according to equation (6).

And by neglecting the stator windings resistance (in the case of for high power generators) the stator voltages equations become

$$V_{ds} = \frac{d\varphi_s}{dt} \qquad (8)$$
$$V_{qs} = \dot{\theta}_s \varphi_s$$

note $\dot{\theta}_s = \omega_s$ and $V_{qs} = V_s$

This gives the following expressions:

$$V_{ds} = 0 \qquad (9)$$
$$V_s = \omega_s \varphi_s$$

The relation between the stator and rotor currents is set from the equation (7)

$$I_{ds} = -\frac{M}{L_s} I_{dr} + \frac{\varphi_s}{L_s} \quad (10)$$
$$I_{qs} = -\frac{M}{L_s} I_{qr}$$

The stator active and reactive powers can be written as:

$$P = V_{ds} I_{ds} + V_{qs} I_{qs} \quad (11)$$
$$Q = V_{qs} I_{ds} - V_{ds} I_{qs}$$

The previous expressions are transformed to the following ones by using equation (9)

$$P = V_s I_{qs} \quad (12)$$
$$Q = V_s I_{ds}$$

and then by using equation (10) the powers are expressed as follows :

$$P = -V_s \frac{M}{L_s} I_{qr} \quad (13)$$
$$Q = -V_s \frac{M}{L_s} I_{dr} + \frac{\varphi_s V_s}{L_s}$$

with $V_s = \omega_s \varphi_s$

so

$$P = -V_s \frac{M}{L_s} I_{qr} \quad (14)$$
$$Q = -V_s \frac{M}{L_s} I_{dr} + \frac{V_s^2}{L_s \omega_s}$$

If the magnetizing inductance M is constant, we note that the active power P is proportional to the quadrature current and reactive power is mainly proportional to the rotor current (4).

To properly control the machine, we will set the relationship between the rotor currents and voltages applied to the machine.

Substituting in equation (3) currents by their value in equations (10) we obtain

$$\varphi_{dr} = \left(L_{r-} \frac{M^2}{L_s}\right) I_{dr} + \frac{V_s^2}{L_s \omega_s} \quad (15)$$
$$\varphi_{qr} = \left(L_{r-} \frac{M^2}{L_s}\right) I_{qr}$$

and replacing the flux in the relation (2) we obtain

$$V_{dr} = R_r I_{dr} + \left(L_{r-} \frac{M^2}{L_s}\right) \frac{dI_{dr}}{dt} - g\omega_s \left(L_{r-} \frac{M^2}{L_s}\right) I_{qr}$$
$$V_{qr} = R_r I_{dr} + \left(L_{r-} \frac{M^2}{L_s}\right) \frac{dI_{qr}}{dt} \quad g\omega_s \left(L_{r-} \frac{M^2}{L_s}\right) I_{qr} + g \frac{V_s^2}{L_s \omega_s} \quad (17)$$

Where g is the slip of the induction machine and

$$\omega_r = g\omega_s$$

In steady state operation the voltage expressions are:

$$V_{dr} = R_r I_{dr} - g\omega_s \left(L_{r-} \frac{M^2}{L_s}\right) I_{qr} \quad (16)$$
$$V_{qr} = R_r I_{dr} + g\omega_s \left(L_{r-} \frac{M^2}{L_s}\right) I_{dr} + g \frac{V_s^2}{L_s \omega_s}$$

It is to be noted from these expressions, one can generate two control strategies. As the powers and voltages are linked by a first order, and in the case where g could be neglected, one can control separately the active and reactive powers. Figure 3 represents a general case where the output depends only on the input without other blocks. So in the direct method we transform figure 4, to match the figure 3.

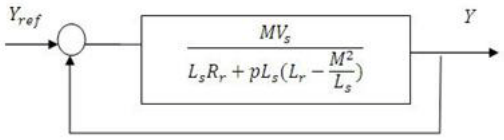

Figure 3: Block diagram of a decoupled relation

The following block diagram represent the different blocks showing the active and reactive powers as outputs and rotor voltages as inputs.

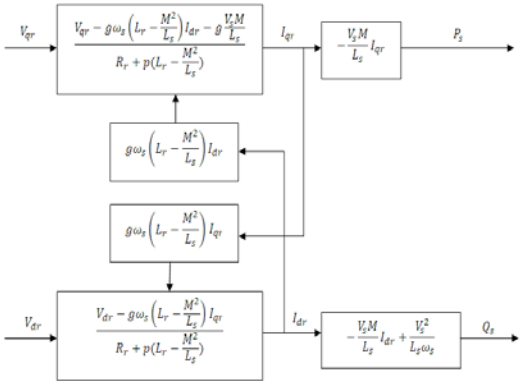

Figure 4: Block diagram of the DFIG taking into account the coupling

3. CONTROL STRATEGIES

In order to decouple the axes d and q, two terms ε_q et ε_d which represent coupling residues and perturbations are introduced. We assume that the term $L_r - \frac{M^2}{L_s}$ could be neglected if we add the constant term ν ($\nu = \frac{V_s^2}{L_s \omega_s}$), figure 5 shows the system after the assumptions considered above [9].

Regulators synthesis:

Both axes can be controlled separately; regulators R_q *et* R_d inputs are P_{ref} - Q_{ref}, and the diphased voltages as outputs. These latter are applied to the generator (DFIG) to allow the wind turbine to rotate at its maximum speed, so a Proportional & Integral Controllers are used. These PI regulators: U(p)/E(s)=$k_p + \frac{k_i}{p}$, followed as it is shown in figure 5 by the following transfer function :

$$H = \frac{MV_s}{L_s R_r + p L_s (L_r - \frac{M^2}{L_s})} \quad (17)$$

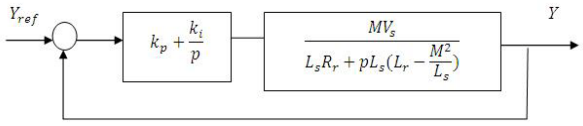

Figure 5: Block diagram for decoupled axes

Determination of parameters k_p *et* k_i *:*
The open loop transfer function is:

$$\boldsymbol{H} = (k_p + \frac{k_i}{p}) * \frac{MV_s}{L_s R_r + p L_s (L_r - \frac{M^2}{L_s})} \quad (18)$$

H can also be written as:

$$\boldsymbol{H} = \frac{(p + \frac{k_i}{k_p})}{\frac{p}{k_p}} * \frac{\frac{MV_s}{L_s\left(L_r - \frac{M^2}{L_s}\right)}}{p + \frac{L_s R_r}{L_s\left(L_r - \frac{M^2}{L_s}\right)}} \quad (19)$$

To eliminate the zeros in this transfer function we use poles compensation. This method is not the only one for the synthesis of a PI controller but it has the advantage to be rapidly implemented in the case of a first order transfer function [8] [9].

$$\frac{k_i}{k_p} = \frac{L_s R_r}{L_s\left(L_r - \frac{M^2}{L_s}\right)} \quad (20)$$

The transfer function becomes:

$$\boldsymbol{H} = \frac{k_p \frac{MV_s}{L_s\left(L_r - \frac{M^2}{L_s}\right)}}{p} \quad (21)$$

The closed loop function is therefore expressed as:

FTBF= $\frac{1}{1+p\tau}$ with

$$\tau = \frac{1}{k_p} \frac{L_s\left(L_r - \frac{M^2}{L_s}\right)}{MV_s} \quad (22)$$

so

$$k_p = \frac{1}{\tau} \frac{L_s\left(L_r - \frac{M^2}{L_s}\right)}{MV_s} \text{ and } k_i = \frac{1}{\tau} \frac{L_s R_r}{MV_s} \quad (23)$$

The term τ is the system response time.

3.1. Indirect control

According to the equations (17), we represent then the system in the following form: [10]:

$$\dot{X} = AX + BU \quad (24)$$
$$Y = CX + DU$$

$$x = \begin{pmatrix} I_{qr} \\ I_{dr} \end{pmatrix}$$

and the rotor voltages are the inputs

$$. e = \begin{pmatrix} Vqr \\ Vdr \end{pmatrix}$$

The state matrix A is as

$$\begin{pmatrix} -\frac{R_r}{\left(L_r - \frac{M^2}{L_s}\right)} & -\frac{g\omega_s\left(L_r - \frac{M^2}{L_s}\right)}{\left(L_r - \frac{M^2}{L_s}\right)} \\ \frac{g\omega_s\left(L_r - \frac{M^2}{L_s}\right)}{\left(L_r - \frac{M^2}{L_s}\right)} & -\frac{R_r}{\left(L_r - \frac{M^2}{L_s}\right)} \end{pmatrix} \quad (25)$$

The control matrix B is in the form

$$\frac{1}{\left(L_r - \frac{M^2}{L_s}\right)} \begin{pmatrix} 1 & 0 \\ 0 & 1 \end{pmatrix} \quad (26)$$

The observation matrix C is the identity matrix ($Y = C * X$), the input-output coupling matrix is zero.

Regulators synthesis:

The goal is to determine a command which allows the poles of the closed loop transfer function to be properly placed [10] according to the desired specifications. The poles of the transfer function are the eigenvalues of the state matrix; the goal is to set a linear state feedback control as it is shown in figure 6. The matrix K is established so that coupling between the currents is neutralized.

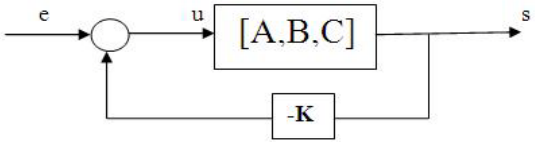

Figure 6: control state feedback

With K= $\begin{pmatrix} k_{11} & k_{12} \\ k_{21} & k_{22} \end{pmatrix}$

The state equation is thus written in the following form:

$$\frac{dx}{dt} = Ax + B(e - Kx) = (A - BK)x + Be \qquad (27)$$

System dynamics is described by the new transfer matrix *L=A-BK*, its eigenvalues are chosen according to the performances demand. So by using the characteristic polynomial P(λ) and resolving the equations system, the matrix K is determined.

$$P(\lambda) = det(\lambda I - A - BK) \qquad (28)$$

$$K = \begin{pmatrix} 1 - R_r & g\omega_s\left(L_r - \frac{M^2}{L_s}\right) \\ g\omega_s\left(L_r - \frac{M^2}{L_s}\right) & 1 - R_r \end{pmatrix} \qquad (29)$$

The resulted control structure is presented in figure 7. The currents I_{qr} and I_{dr} are decoupled and defined using two PI power regulators..

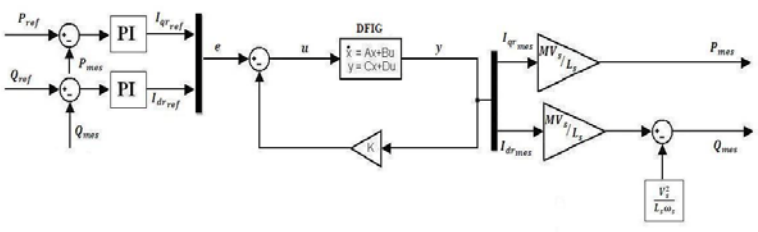

Figure 7: Indirect control structure

3.2. Performance analysis

This section gives the comparison simulation results between the two control strategies in term of robustness and performances. For these simulations a Double Fed Induction Generator of 1.5 KW is considered.

a- Following up the control signal:

In this first test step variations of active and reactive powers are applied while the machine is driven at fixed speed.

Test conditions:

Machine trained at 1450 rpm

at t = 3s: P_{ref} goes from 0 to -2000W
at t = 2s: Q_{ref} goes from 0 to 1000 VAR

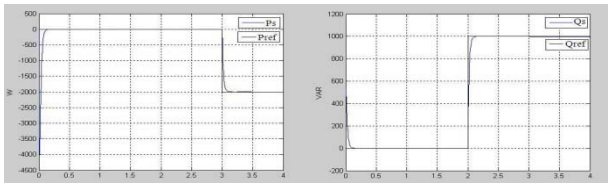

Figure 8: reference tracking active power and reactive (direct control)

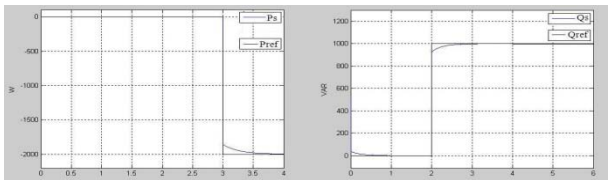

Figure 9: reference tracking of active and reactive power (indirect control)

b- Sensitivity to disturbances:

This test enables us to verify the behavior of output powers when the rotational speed of the machine varies abruptly.
Test conditions:
machine being driven at 1350 rpm
active power setpoint fixed at -1000 W
fixed reactive power setpoint fixed at 1000 VAR
at t = 2s speed changes suddenly from 1350 to 1450 rpm.

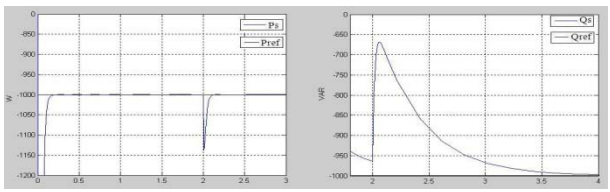

Figure 10: Effect on powers of a sudden change in speed (direct control)

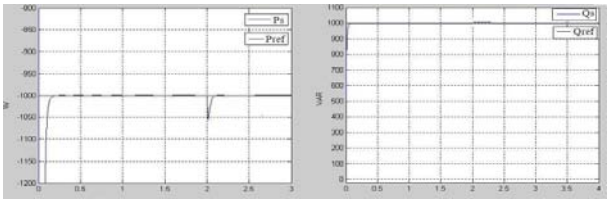

Figure 11: Effect on the powers of a sudden change in speed (indirect control)

c- Robustness:

To test robustness, we vary the model parameters of the used DFIG. In fact in the calculations of regulators constants, the different parameters are assumed fixed. Or in a real system, these parameters can vary due to different physical phenomena (inductor saturation resistance heat etc…), and also due to measurements inaccuracies.

Test conditions:

t = 2s: resistors R_s and R_r multiplied by 2
the inductance L_s, $L_r$and M divided by 2
machine being driven at 1350 rpm.
at t = 3.5 s: Q_{ref} goes from 0 to -1000 VAR
at t = 3.5 s: P_{ref}goes from 0 to 1000W

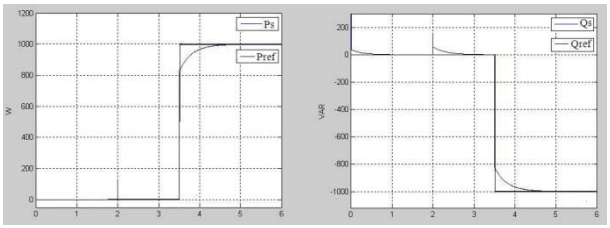

Figure 12: Effect of DFIG parameter variations on P_s and Q_s (indirect control)

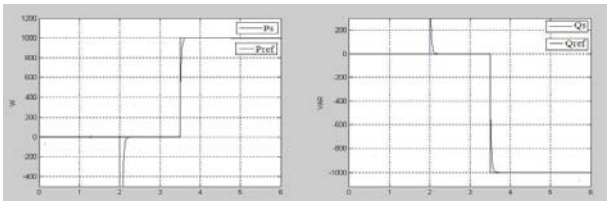

Figure 13: Effect of DFIG parameter variations on P_s and Q_s (direct control)

It is to be noted that rotation speed variation and the generator parameters change have a weak impact on indirect control method. This control development has enabled us to highlight several interesting aspects for further study on the whole power wind production. It is obvious that direct method is easier to implement than the indirect one. According to the simulation results the indirect method is more robust and less sensitive to perturbations.

CONCLUSION

The purpose of this work is to investigate control approaches of a Double Fed Induction Generator: a direct control without taking into account the coupling between the present currents and an indirect control based on state space approach. A comparison in term of robustness and stability between the two methods is presented through simulation results.

As the whole presented work is based upon simulation, we are currently working on an experimental bench [12] in order to validate experimentally the obtained simulation results. As a future work, we intend to propose a real-time implementation of the proposed control using the system model and Real-Time Workshop using dSPACE hardware.

REFERENCES

[1] A.MIRECKI, "*Etude comparative de chaînes de conversion d'énergie dédiées à une éolienne de petite puissance*", thèse 2005
[2] B.Beltran, " *Maximisation de la puissance produite par une génératrice asynchrone Double alimentation d'une éolienne par mode glissant d'ordre supérieur*", JCGE'08 Lyon 17&18/12/08
[3] B.Boukhezzar, "*Sur les stratégies de commande pour l'optimisation et la régulation de puissance des éoliennes a vitesse variable*", thèse 2006
[4] Shashikanth Suryanarayanan and Amit Dixit, "*Control of Large Wind Turbines: Review and Suggested Approach to Multivariable Design*"
[6] H. Razik, "*Modélisation de la machine asynchrone à cage. Application à la simulation de moteurs à cage défaillante. Spectres des courants des moteurs défaillants*", Université Henry Poincaré
[7] L.C.Henriksen, "*Model Predictive Control of a Wind Turbine*", Technical University of Denmark 2007
[8]A.Boyette, "*Contrôle-commande d'un générateur asynchrone a double alimentation avec système de stockage pour la production éolienne*", thèse 2006
[9] Fréderic Poitiers, "*Etude et commande de génératrice asynchrones pour l'utilisation de l'énergie éolienne*", école polytechnique de l'université de Nantes 2003
[10] Philipe de Larminat, *"Automatique: commande des systems lineaire"* Edition Hermes 1996
[11] Holdsworth L, Wu XG, Ekanayake JB, Jenkins N. *Comparison of fixed speed and doubly-fed induction wind turbines during power system disturbances*. IEE Proceedings: Generation, Transmission, Distribution, 2003, 3: 343-352.
[12] A.Naamane, N.K M'sirdi "MACSyME: Modelling, Analysis and Control for Systems with Multiple Energy sources" , *in : Springer , "Book Proceeding of SEB 2009", Springer Berlin Heidelberg, Vol. ISBN 978-3-642-03453-4 , Ch. Sustainability in Energy and Buildings,http://www.springerlink.com/content/v23046h301v7015n/* Mai 2009 .